

DOI: 10.1002/adma.200702145

# High-Performance Air-Stable Bipolar Field-Effect Transistors of Organic Single-Crystalline Ribbons with an Air-Gap Dielectric\*\*

By Qingxin Tang, Yanhong Tong, Hongxiang Li,\* Zhuoyu Ji, Liqiang Li, Wenping Hu,\* Yunqi Liu, and Daoben Zhu

Bipolar organic field-effect transistors (OFETs) have attracted considerable interest for realizing complementary-like organic integrated circuits, which operate with low power dissipation, wide noise margins, and great operational stability.<sup>[1]</sup> However, until recently, there have been few reports on achieving bipolar OFET operation. A main challenge is the efficient injection of both charge carriers.<sup>[1]</sup> For most organic semiconductors, the ionization potential (the highest occupied molecular orbital (HOMO) level) has the same order of magnitude as the work functions,  $\phi$ , of the usually used metal electrodes (for example, for Au  $\phi \approx 5.2$  eV). As a result, the barrier for hole injection is small, but the barrier for electron injection is large, such that the device cannot exhibit n-type operation. Doping or defect accommodation on the surface of an organic semiconductor probably further alters the barrier for carrier injection, especially for electrons. Using narrow-band-gap semiconductors, low-work-function metals, or asymmetric electrodes can reduce the injection barriers.<sup>[2]</sup> However, the number of the narrow-band-gap organic semiconductors is very limited. There are still few metals of which the work functions match with the electron affinity (the lowest unoccupied molecular orbital (LUMO) level) of organic semiconductors. Further, these metals are generally unstable (e.g., Ca and Mg). The deposition of the asymmetric electrodes is relatively complex. Therefore, it is difficult for researchers to find really effective ways to solve this problem. Another challenge for the realization of bipolar transport is the trapping of one or both carriers.<sup>[1]</sup> For example, electrons are likely to

be trapped by impurities, moisture, oxygen, or the hydroxyl groups of the dielectric.<sup>[3]</sup> As a result, the electron mobilities are generally much smaller than the hole mobilities in bipolar devices. These trapping effects can be weakened or prevented by using highly pure materials, processing in an inert atmosphere, and using a hydroxyl-free dielectric.<sup>[3a]</sup> However, the rigorous operation environment enhances the difficulty of organic-device-physics research and applications. Therefore, air-stable bipolar OFETs are an important issue in organic electronics. Finally, high charge mobility is required in all organic transistors in order to build electronic circuits with high-frequency operation.<sup>[4]</sup> However, owing to the above-mentioned difficulties such as for effective injection and transport of both carriers in bipolar OFETs, most devices show low hole and electron mobilities in the  $10^{-4}$  to  $10^{-3}$  cm<sup>2</sup> V<sup>-1</sup> s<sup>-1</sup> range, which are even lower than those values in the corresponding unipolar OFETs.<sup>[1]</sup> As a result, low mobility is still a limitation for bipolar OFETs.

Our laboratory has been concentrating on OFETs for some years<sup>[5]</sup> and has acknowledged the problems of bipolar OFETs encountered. We believe, for the fundamental investigation, as well as for the practical application of bipolar OFETs, it is imperative (i) to find candidates for organic semiconductors with high mobility, good air stability, and efficient carrier injection for both electrons and holes; and (ii) to eliminate the serious trapping of electrons and holes in the insulating dielectric materials or at the interface between the gate dielectric and organic semiconductor.

Phthalocyanines have attracted attention in OFETs for some years because of their remarkable chemical and thermal stabilities as well as their non-toxicity and good field-effect mobilities.<sup>[6]</sup> For example, the electron mobility of copper-hexadecafluoro-phthalocyanine (F<sub>16</sub>CuPc), an air-stable n-type organic semiconductor that first received attention by Bao et al.,<sup>[6c]</sup> was demonstrated to be as high as 0.2 cm<sup>2</sup> V<sup>-1</sup> s<sup>-1</sup>.<sup>[5f]</sup> Copper phthalocyanine (CuPc) exhibited the highest hole mobility near 1.0 cm<sup>2</sup> V<sup>-1</sup> s<sup>-1</sup>.<sup>[6d]</sup> Moreover, the electron affinity of F<sub>16</sub>CuPc was 4.7–4.8 eV and the ionization potential of CuPc was 5.0–5.2 eV: they were similar to the work function of the commonly used electrode material, Au, for efficient carrier injection. Therefore, it is prospective to realize the efficient injection of both electrons and holes in bipolar transistors based on CuPc and F<sub>16</sub>CuPc with Au as the drain and source electrodes (Figure 1a).

[\*] Dr. H. Li, Prof. W. Hu, Dr. Q. Tang, Dr. Y. Tong, Z. Ji, L. Li, Prof. Y. Liu, Prof. D. Zhu  
Beijing National Laboratory for Molecular Sciences  
Key Laboratory of Organic Solids  
Institute of Chemistry, Chinese Academy of Sciences  
Beijing 100080 (P.R. China)  
E-mail: lhx@iccas.ac.cn; huwp@iccas.ac.cn  
Dr. Q. Tang, Z. Ji, L. Li  
Graduate School of Chinese Academy of Sciences  
Beijing 100039 (P.R. China)

[\*\*] The authors acknowledge financial support from the National Natural Science Foundation of China (20421101, 20404013, 20571079, 50725311), the Ministry of Science and Technology of China (2006CB806200, 2006CB932100), and the Chinese Academy of Sciences.

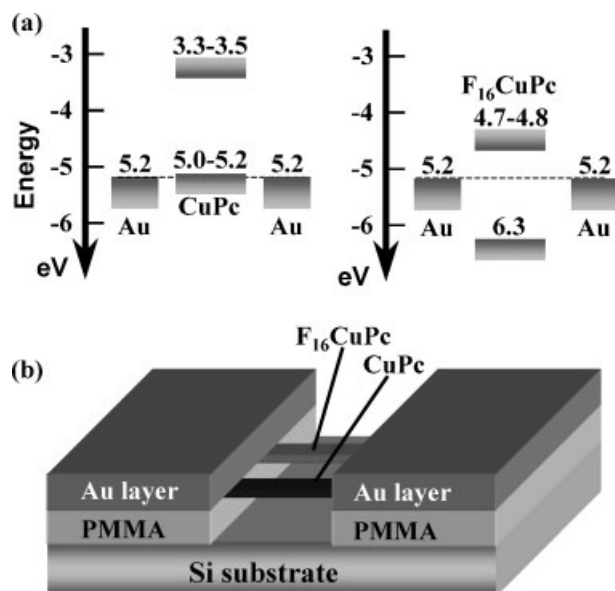


**Figure 1.** a) Energy levels of CuPc and F<sub>16</sub>CuPc and work function of Au. b) Schematic structure of an air-dielectric bipolar transistor based on CuPc and F<sub>16</sub>CuPc single-crystalline sub-micrometer ribbons.

Rogers and Podzorov et al.<sup>[7]</sup> introduced an unusual device design by replacing the standard solid dielectric layer with a thin free-space gap that can be occupied by air, nitrogen, other gases, or even vacuum. Unlike the effects associated with electric contacts, the free-space dielectric simply eliminates the trapping of electrons and holes in the dielectric and at the interface between the dielectric and semiconductor by eliminating the solid dielectric material. Morpurgo et al.<sup>[8]</sup> found that a free-space dielectric provides a pristine interface to reduce the interface defects and minimize the Fröhlich polaron effect. This is uniquely well-suited to the study of organic semiconductors, which do not possess the types of dangling bonds or surface states that exist at the interface between a gate dielectric and organic semiconductor. For example, it enabled realization of intrinsic polaronic transport<sup>[9]</sup> and the observation of the Hall effect in the field-induced accumulation layer on the surface of rubrene single crystals.<sup>[10]</sup> Very recently, based on the same device configuration, high-performance single-crystalline transistors of tetracene have also been fabricated and the pronounced crystal anisotropy in the mobility was examined by Frisbie et al.<sup>[11]</sup>

Combining the advantages of the similar energy levels of CuPc and F<sub>16</sub>CuPc to Au electrodes, the good stability and high mobilities of CuPc and F<sub>16</sub>CuPc, and the great advantages of free-space dielectrics for the

investigation of organic semiconductors, here, a series of bipolar transistors were fabricated by using the air-gap dielectric technique based on single-crystalline sub-micrometer ribbons of CuPc and F<sub>16</sub>CuPc (see Fig. 1b). The bipolar devices showed excellent air-stable characteristics with electron and hole mobilities as high as 0.17 and 0.1 cm<sup>2</sup> V<sup>-1</sup> s<sup>-1</sup>, respectively. The symmetrical bipolar characteristics, the high electron and hole mobilities, and the excellent air stability indicate the potential applications of the bipolar devices in organic integrated circuits.

Single-crystalline sub-micrometer-sized ribbons of F<sub>16</sub>CuPc and CuPc were produced by the physical vapor transport technique as previously described.<sup>[5d-f]</sup> Device fabrication was performed on a Micromanipulator 6150 probe station. Figure 2 shows the fabrication process of the bipolar device, which can be divided into four distinct stages: (i) the polymer layer of poly(methyl methacrylate) (PMMA) (in chlorobenzene) is spin-coated onto a Si substrate (Fig. 2a), (ii) a gap of several micrometers wide is created by using the tip of a mechanical probe to scratch the PMMA layer under a microscope (Fig. 2b), (iii) the individual single-crystalline sub-micrometer-sized ribbons are transferred and bridge the gap (Fig. 2c-d); and (iv) the thin Au layers are glued onto the sub-micrometer ribbons by the van der Waals force with the help of the mechanical probes (Fig. 2e-f). The Au layers were prepared as follows: firstly, Au thin film with a thickness of ~100 nm was predeposited on a Si wafer by thermal evaporation. Then, a small piece of the Au film, approximately 30 × 150 μm<sup>2</sup>, was peeled off the Si substrate with the tip of the mechanical probe and transferred onto the sub-micrometer-sized ribbons as a source or drain electrode (Fig. 2e-f). The Si substrate

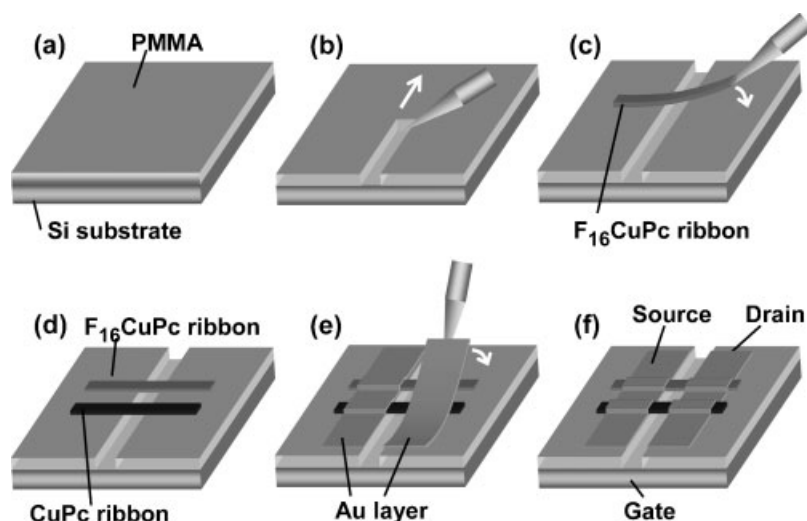


**Figure 2.** Bipolar single-crystalline device fabrication: a) A PMMA layer is spin-coated onto a Si substrate. b) A gap of micrometer width is created by using the tip of a mechanical probe to scratch the PMMA layer. c-d) Individual ribbons of CuPc and F<sub>16</sub>CuPc, respectively, are transferred onto the PMMA layer. e-f) The Au layers are transferred onto the ribbon as the source and drain electrodes. The Si substrate functions as the gate electrode. The gap is naturally filled with air, which serves as the gate dielectric. The arrows show the movement directions of the probes.

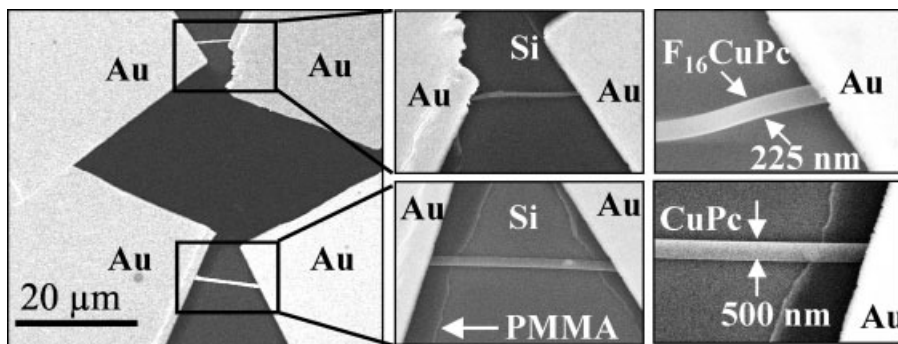


**Figure 3.** SEM images of a representative bipolar device of the single-crystalline ribbons of CuPc and F<sub>16</sub>CuPc, the air served as the gate dielectric.

functioned as the gate electrode. The gap was naturally filled with air, which served as the gate dielectric. Certainly, the bipolar devices could also be fabricated by the integration of two individual unipolar devices of CuPc and F<sub>16</sub>CuPc.

A typical bipolar device fabricated by the technique based on single-crystalline ribbons of CuPc and F<sub>16</sub>CuPc is shown in Figure 3. The widths of the CuPc and F<sub>16</sub>CuPc ribbons were around 500 nm and 225 nm, respectively. The PMMA thickness was around 350 nm, thus the thickness of the air-gap dielectric was around 350 nm. Au was used as the source and drain electrodes for similar energy levels between the electrodes and the organic semiconductors.

Figure 4 shows the output characteristics of the bipolar device measured in air at room temperature. At high gate voltage  $|V_G|$  and low source-drain voltage  $|V_{SD}|$ , the device worked as a unipolar transistor in electron- or hole-accumulation mode. At low  $|V_G|$  (0–6 V) and the relative, higher  $|V_{SD}|$ , the electrons and holes were accumulated in their respective channels, causing a pronounced increase of the current  $|I_{SD}|$  with the increasing  $|V_{SD}|$ , which confirmed the occurrence of its bipolar operation.

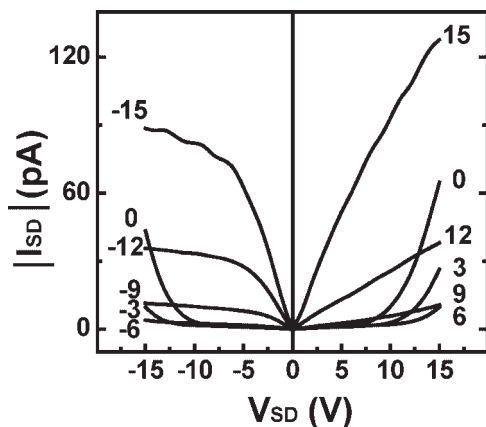


**Figure 4.** Output curves of a bipolar air-dielectric OFET device based on CuPc and F<sub>16</sub>CuPc sub-micrometer ribbons. The gate voltage  $|V_G|$  changed from 0 to 15 V.

The transfer characteristics of the bipolar device are shown in Figure 5a. For comparison, the curves of the unipolar devices of CuPc and F<sub>16</sub>CuPc fabricated with the same method are given in Figure 5b and c, respectively, where the depletion modes can be clearly observed at low  $|V_G|$ . The transfer curves in Figure 5a show the V-shaped characteristics, which confirmed the efficient bipolar behavior, with one arm for electron transport and the other for hole transport. According to the transfer curves of the bipolar device at  $|V_{SD}| = 20$  V, the hole and electron mobilities were

calculated at ca. 0.1 and ca. 0.17 cm<sup>2</sup> V<sup>-1</sup> s<sup>-1</sup>, respectively. These values are nearly two orders of magnitude higher than those of bipolar transistors of CuPc and F<sub>16</sub>CuPc thin films (with highest bipolar mobilities at  $3.3 \times 10^{-3}$  cm<sup>2</sup> V<sup>-1</sup> s<sup>-1</sup> for both electrons and holes).<sup>[12]</sup> The reasons are probably assigned to (i) the high-quality single crystals significantly reducing disorder and defect density,<sup>[13]</sup> and (ii) the air

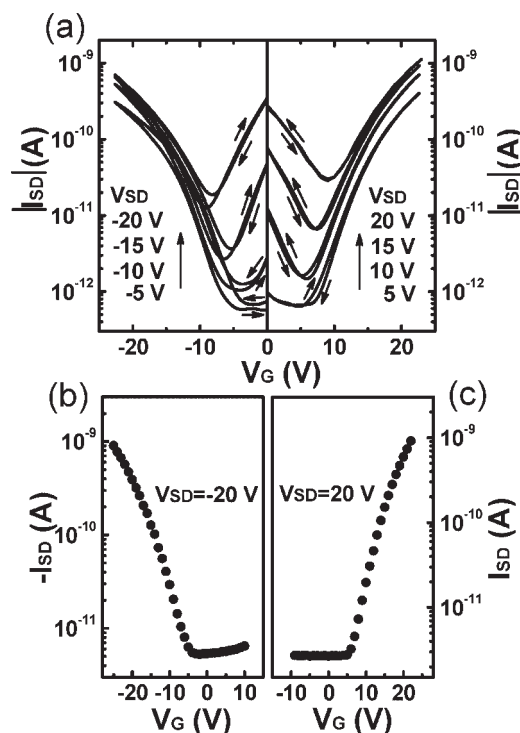


**Figure 5.** Transfer curves of the air-dielectric devices: a) Bipolar device of CuPc and F<sub>16</sub>CuPc ribbons. b) Unipolar p-type device of an individual CuPc ribbon. c) Unipolar n-type device of an individual F<sub>16</sub>CuPc ribbon. The arrows show the sweep directions. For the CuPc ribbon, channel length  $L = 10.6$  μm, channel width  $W = 500$  nm. For the F<sub>16</sub>CuPc ribbon,  $L = 5.6$  μm,  $W = 225$  nm. According to the curves at  $|V_{SD}| = 20$  V, the obtained mobilities  $\mu$  are as follow: a)  $\mu_h \approx 0.1$  cm<sup>2</sup> V<sup>-1</sup> s<sup>-1</sup>,  $\mu_e \approx 0.17$  cm<sup>2</sup> V<sup>-1</sup> s<sup>-1</sup>. b)  $\mu_h \approx 0.1$  cm<sup>2</sup> V<sup>-1</sup> s<sup>-1</sup>. c)  $\mu_e \approx 0.17$  cm<sup>2</sup> V<sup>-1</sup> s<sup>-1</sup>.

dielectric providing a pristine interface between the crystal and gate dielectric to decrease the interface defects.<sup>[7–10,14]</sup> To the best of our knowledge, this was in a class with the highest mobility for bipolar OFETs reported so far.<sup>[1]</sup> In particular, the electron mobility may be the highest among bipolar organic transistors.<sup>[1]</sup>

The attractive point of our bipolar transistors was the good balanced injection of electrons and holes as shown in Figure 4 and Figure 5a. As we know, until now, bis(ethylenedithio)-tetrathiafulvalene, CuPc, iron phthalocyanine (FePc) and rubrene single crystals, for example, have been applied in bipolar transistors.<sup>[15]</sup> In the devices, the electron mobilities were always 2–3 orders lower than their hole mobilities. The remarkable unbalanced mobilities were a main problem for these bipolar OFETs. In our devices, the effective bipolar mobilities for holes and electrons were high and at the same level, which can be assigned to the high and similar mobilities in unipolar devices of single-crystalline ribbons of CuPc and F<sub>16</sub>CuPc (as shown in Fig. 5b and c).

Compared with the previously-reported unipolar SiO<sub>2</sub>-dielectric devices with Au as the source and drain electrodes (0.1–0.4 cm<sup>2</sup> V<sup>−1</sup> s<sup>−1</sup> in CuPc devices and 0.01 cm<sup>2</sup> V<sup>−1</sup> s<sup>−1</sup> in F<sub>16</sub>CuPc devices, respectively),<sup>[5d–f]</sup> the hole mobility of the air-dielectric devices remained similar while the electron mobility increased by over one order. This confirms that the air-gap dielectric has a high possibility of eliminating the serious trapping of electrons by eliminating the insulating dielectric material, so that a pristine interface between the crystal and the gate dielectric can be obtained.<sup>[8]</sup> The same-level hole mobilities using SiO<sub>2</sub> and air as the dielectric further proved that (i) electrons are more strongly trapped than holes in SiO<sub>2</sub> dielectric devices, and (ii) our previously fabricated SiO<sub>2</sub> dielectric devices based on single-crystalline CuPc ribbons had a good dielectric/semiconductor interface; that is to say the commonly used Si/SiO<sub>2</sub> substrates should be applicable for the investigation of p-type organic semiconductors, and are not the best candidate for n-type organic semiconductors. In this case, by applying an air dielectric to substitute the solid SiO<sub>2</sub> dielectric, the electron-trapping effect can be reduced so that the mobility of organic semiconductors can be increased remarkably.

In some reports considerable hysteresis has been observed in bipolar transistors during the transfer-characteristics sweeps,<sup>[16]</sup> which has been attributed to charge-trapping effects at the semiconductor/dielectric interface or in the bulk of the dielectric.<sup>[17]</sup> Compared with these devices, the transfer curves of our devices showed very weak hysteresis (Fig. 5a), which further confirms the advantage of an air dielectric in reducing the charge-trapping effects. Moreover, our bipolar OFETs exhibited good air stability, which has been observed only in very few organic bipolar devices.<sup>[2b,12b,18]</sup> The excellent air stability of the devices indicated their ease in processing and operation conditions for the building of organic integrated circuits.

Finally, it should be addressed that the air-gap technique presents an all-dry manufacturing process except in the spin-

coating of the PMMA layer. It not only avoids the use of toxic or environmentally harmful solvents,<sup>[19]</sup> but also effectively avoids wrinkles of the Au layer and the degradation in the device performance.<sup>[13,20]</sup> In addition, this technique eliminated the solid dielectric material, which simplified the process of device fabrication and provided a way to characterize organic semiconductors more effectively. As we know, one main challenge for the fabrication of organic single-crystalline OFETs is electrical contact. The conventional method for electrode fabrication is metal deposition on the single crystal and/or on the dielectric by evaporation or sputtering. On the one hand, because of the fragility of the organic materials, high-temperature and high-energy metal atoms will seriously damage the crystalline surface and degrade the device performance.<sup>[21]</sup> On the other hand, in the process of the metal deposition, the metal atoms easily fill the pinholes in the dielectric, causing high current leakages.<sup>[20]</sup> This may conceal the properties of the organic materials, and may even cause a failure in the measurement of the electrical properties of organic devices, in particular, small-sized organic crystal devices.<sup>[22]</sup> Our device fabrication process does not involve metal deposition, and hence can effectively overcome this challenge, to offer a feasible approach of avoiding thermal-radiation damage on the crystal and minimizing the problem of pinholes. The leakage current in our devices is of the order of 10<sup>−14</sup>–10<sup>−13</sup> A at V<sub>G</sub> = 20 V, which is over four orders of magnitude lower than the current *I*<sub>SD</sub>.

In conclusion, aiming at the challenges of organic bipolar OFETs (such as the unbalanced mobilities and injection of both electrons and holes, the serious trapping of electrons and holes by the insulating dielectric materials or the interface between the gate dielectric and organic semiconductor), high-performance bipolar OFETs were fabricated by using single-crystalline sub-micrometer-sized ribbons of CuPc and F<sub>16</sub>CuPc and the air-gap dielectric. The similar energy levels of CuPc and F<sub>16</sub>CuPc to the work function of the Au electrodes, the high mobility of CuPc and F<sub>16</sub>CuPc single crystals, and the great advantages of the air-gap dielectric resulted in a high performance of the bipolar devices. The devices showed excellent air-stable characteristics with electron and hole mobilities as high as 0.17 and 0.1 cm<sup>2</sup> V<sup>−1</sup> s<sup>−1</sup>, respectively. The balanced bipolar characteristics, the high electron and hole mobilities, and the excellent air stability indicate the potential applications of these bipolar devices in organic integrated circuits.

## Experimental

CuPc and F<sub>16</sub>CuPc sub-micrometer ribbons were synthesized by physical vapor transport processes as previously described.<sup>[5d–f]</sup> The materials were purified three times by thermal-gradient sublimation prior to processing. Ar was used as the carrier gas. The system was evacuated to avoid oxidation of the materials and to decrease the source evaporation temperature. The source temperatures were ca. 425 °C for CuPc, and ca. 400 °C for F<sub>16</sub>CuPc, respectively. The deposition time was 1 h. The device fabrication process was mainly carried out with a Micromanipulator 6150 probe station. PMMA in chlorobenzene was spin-coated onto a Si substrate followed by thermal



annealing at 100 °C for 5 min. The thickness of the PMMA layer was ca. 350 nm, as measured using an Ambios Technology XP-2 surface profilometer. The current-voltage (*I*-*V*) characteristics of the OFETs were measured with the Micromanipulator 6150 probe station in a clean and metallic shielded box at room temperature in air, and recorded using a Keithley 4200 SCS. SEM images were obtained with a Hitachi S-4800 SE (Japan).

Received: August 25, 2007

Revised: October 15, 2007

Published online: April 1, 2008

- [1] J. Zaumseil, H. Sirringhaus, *Chem. Rev.* **2007**, *107*, 1296.
- [2] a) E. J. Meijer, D. M. de Leeuw, S. Setayesh, E. van Veenendaal, B.-H. Huisman, P. W. M. Blom, J. C. Hummelen, U. Scherf, T. M. Klapwijk, *Nat. Mater.* **2003**, *2*, 678. b) T. D. Anthopoulos, S. Setayesh, E. Smits, M. Cölle, E. Cantatore, B. de Boer, P. W. M. Blom, D. M. de Leeuw, *Adv. Mater.* **2006**, *18*, 1900. c) E. C. P. Smits, T. D. Anthopoulos, S. Setayesh, E. van Veenendaal, R. Coehoorn, P. W. M. Blom, B. de Boer, D. M. de Leeuw, *Phys. Rev. B: Condens. Matter* **2006**, *73*, 205316. d) C. Rost, D. J. Gundlach, S. Karg, W. Riess, *J. Appl. Phys.* **2004**, *95*, 5782. e) R. Schmechel, M. Ahles, H. von Seggern, *J. Appl. Phys.* **2005**, *98*, 084511.
- [3] a) L. Chua, J. Zaumseil, J. Chang, E. C.-W. Ou, P. K.-H. Ho, H. Sirringhaus, R. H. Friend, *Nature* **2005**, *434*, 194. b) R. G. Kepler, *Phys. Rev.* **1960**, *119*, 1226.
- [4] J. Cornil, J. Bredas, J. Zaumseil, H. Sirringhaus, *Adv. Mater.* **2007**, *19*, 1791.
- [5] a) W. Hu, Y. Liu, Y. Xu, S. Liu, S. Zhou, D. Zhu, *Synth. Met.* **1999**, *104*, 19. b) K. Xiao, Y. Liu, P. Hu, G. Yu, X. Wang, D. Zhu, *Appl. Phys. Lett.* **2003**, *83*, 150. c) Y. Sun, Y. Liu, D. Zhu, *J. Mater. Chem.* **2005**, *15*, 53. d) Q. Tang, H. Li, M. He, W. Hu, C. Liu, K. Chen, C. Wang, Y. Liu, D. Zhu, *Adv. Mater.* **2006**, *18*, 65. e) Q. Tang, H. Li, Y. Song, W. Xu, W. Hu, L. Jiang, Y. Liu, X. Wang, D. Zhu, *Adv. Mater.* **2006**, *18*, 3010. f) Q. Tang, H. Li, Y. Liu, W. Hu, *J. Am. Chem. Soc.* **2006**, *128*, 14634. g) Q. Tang, L. Li, Y. Song, Y. Liu, H. Li, W. Xu, Y. Liu, W. Hu, D. Zhu, *Adv. Mater.* **2007**, *19*, 2624.
- [6] a) J. Simon, J. J. Andre, *Molecular Semiconductors: Photoelectrical Properties and Solar Cells*, Springer, Berlin **1985**, Ch. 1.[b] *Phthalocyanines: Properties and Applications*, Vol. 3, (Eds: C. C. Leznoff, A. B. P. Lever), VCH, Weinheim, Germany **1993**, Ch. 1.[c] Z. Bao, A. J. Lovinger, J. Brown, *J. Am. Chem. Soc.* **1998**, *120*, 207. d) R. Zeis, T. Siegrist, C. Kloc, *Appl. Phys. Lett.* **2005**, *86*, 022103.
- [7] E. Menard, V. Podzorov, S. Hur, A. Gaur, M. E. Gershenson, J. A. Rogers, *Adv. Mater.* **2004**, *16*, 2097.
- [8] I. N. Hulea, S. Fratini, H. Xie, C. L. Mulder, N. N. Iossad, G. Rastelli, S. Ciuchi, A. F. Morpurgo, *Nat. Mater.* **2006**, *5*, 982.
- [9] V. Podzorov, E. Menard, A. Borissov, V. Kiryukhin, J. A. Rogers, M. E. Gershenson, *Phys. Rev. Lett.* **2004**, *93*, 086602.
- [10] V. Podzorov, E. Menard, J. A. Rogers, M. E. Gershenson, *Phys. Rev. Lett.* **2005**, *95*, 226601.
- [11] Y. Xia, V. Kalihari, C. D. Frisbie, N. K. Oh, J. A. Rogers, *Appl. Phys. Lett.* **2007**, *90*, 162106.
- [12] a) J. Wang, H. B. Wang, X. J. Yan, H. C. Huang, D. H. Yan, *Appl. Phys. Lett.* **2005**, *87*, 093507. b) J. Wang, H. B. Wang, X. J. Yan, H. C. Huang, D. H. Yan, *Chem. Phys. Lett.* **2005**, *407*, 87. c) R. Ye, M. Baba, K. Mori, *Jpn. J. Appl. Phys.* **2005**, *44*, 581. d) R. Ye, M. Baba, Y. Oishi, K. Mori, K. Suzuki, *Appl. Phys. Lett.* **2005**, *86*, 253505. e) J. Wang, H. Wang, X. Yan, H. Huang, D. Jin, J. W. Shi, Y. Tang, D. Yan, *Adv. Funct. Mater.* **2006**, *16*, 824.
- [13] C. Reese, Z. Bao, *Mater. Today* **2007**, *10*, 20.
- [14] a) Z. Bao, V. Kuck, J. A. Rogers, M. A. Paczkowski, *Adv. Funct. Mater.* **2002**, *12*, 526. b) R. W. I. de Boer, M. Jochemsen, T. M. Klapwijk, A. F. Morpurgo, J. Niemax, A. K. Tripathi, J. Pflaum, *J. Appl. Phys.* **2004**, *95*, 1196. c) H. E. Katz, Z. Bao, *J. Phys. Chem. B* **2000**, *104*, 671.
- [15] a) T. Hasegawa, K. Mattenberger, J. Takeya, B. Batlogg, *Phys. Rev. B: Condens. Matter* **2004**, *69*, 245115. b) R. W. I. de Boer, A. F. Stassen, M. F. Craciun, C. L. Mulder, A. Molinari, S. Rogge, A. F. Morpurgo, *Appl. Phys. Lett.* **2005**, *86*, 262109. c) T. Takahashi, T. Takenobu, J. Takeya, Y. Iwasa, *Appl. Phys. Lett.* **2006**, *88*, 033505.
- [16] a) T. B. Singh, F. Meghdadi, S. Gunes, N. Marjanovic, G. Horowitz, P. Lang, S. Bauer, N. S. Sariciftci, *Adv. Mater.* **2005**, *17*, 2315. b) A. Opitz, M. Bronner, W. Brutting, *J. Appl. Phys.* **2007**, *101*, 063709.
- [17] N. Marjanović, T. B. Singh, G. Dennler, S. Gunes, H. Neugebauer, N. S. Sariciftci, R. Schwodiauer, S. Bauer, *Org. Electron.* **2006**, *7*, 188.
- [18] H. Wang, J. Wang, X. Yan, J. Shi, H. Tian, Y. Geng, D. Yan, *Appl. Phys. Lett.* **2006**, *88*, 133508.
- [19] H. Klauk, U. Zschieschang, J. Pflaum, M. Halik, *Nature* **2007**, *445*, 745.
- [20] a) K. T. Shimizu, J. D. Fabbri, J. J. Jelencic, N. A. Melosh, *Adv. Mater.* **2006**, *18*, 1499. b) A. Vilan, D. Cahen, *Adv. Funct. Mater.* **2002**, *12*, 795.
- [21] a) V. Podzorov, V. M. Pudalov, M. E. Gershenson, *Appl. Phys. Lett.* **2003**, *82*, 1739. b) M. A. Rampi, G. M. Whitesides, *Chem. Phys.* **2002**, *281*, 373.
- [22] R. W. I. de Boer, N. N. Iosad, A. F. Stassen, T. M. Klapwijk, A. F. Morpurgo, *Appl. Phys. Lett.* **2005**, *86*, 032103.